



## Investigating the Potential of Vertical-TEC as an Earthquake Precursor: Haiti Major ( $M_L$ 7) Earthquake Case Study

Marjan Mohammed Ghafar<sup>1\*</sup>, Sarkhel Dleer<sup>1</sup>, Sebar Mukhtar<sup>1</sup>, Dawar HK Mohammed<sup>1</sup>, Hemn Mohammed Salh<sup>2</sup>

<sup>1</sup>Department of Physics, College of Science, University of Halabja, Halabja, Kurdistan Region, Iraq.

<sup>2</sup>Department of Physics, Faculty of Science and Health, Koya University, Koya, Erbil, Kurdistan Region, Iraq.

Received 16 November 2023; revised 20 April 2024;  
accepted 23 April 2024; available online 05 May 2024

DOI: 10.24271/PSR.2024.425626.1421

### ABSTRACT

This study explores whether vertical total electron content (VTEC or TEC) can serve as a precursor to a major earthquake (magnitude 7) that occurred in Haiti on January 12, 2010. The analysis involves examining and correlating various ionospheric and atmospheric parameters. Two TEC data stations are utilized: Scub, located approximately 377.80 km from the epicentre within the earthquake preparation zone (EPZ), and Cro1, situated about 847.7 km from the epicentre outside the EPZ by applying the mean and standard deviation methods. The study reveals a noteworthy finding: a positive TEC anomaly of about 13 TECU was identified at the Scub station, only 11 days before the main earthquake event. This positive anomaly can be credited as a potential precursor, as it persists even after mitigating the impact of external factors such as geomagnetic storms and atmospheric parameters. Furthermore, the positive TEC anomaly is localized, as it was not observed outside the EPZ at the Crol station.

<https://creativecommons.org/licenses/by-nc/4.0/>

*Keywords:* Seismo-Ionospheric Coupling; Radon Emissions; Earthquake Forecasting; Geomagnetic Activity; TEC Anomalies; Enriquillo Plantain Garden Fault Zone.

### 1. Introduction

Despite scientific progress, earthquake prediction remains elusive<sup>[1, 2]</sup>. Various methods exist, but none are universally reliable<sup>[3]</sup>. Scientists strive to devise an effective approach to preserving lives and minimizing the repercussions of seismic disasters<sup>[4-6]</sup>. The domain of earthquake physics encompasses a multifaceted and extensive area of study<sup>[7,8]</sup>. Spanning various facets of the Earth's crustal composition, commencing with the dynamics of tectonic plates and ending in the intricate microscopic mechanisms governing friction, chemical reactions, and electric charge generation<sup>[9, 10]</sup>. For this complex topic to be properly looked at, it is essential to combine knowledge from a variety of fields, such as seismology, atmospheric and ionospheric physics, as well as geomagnetic activity<sup>[11]</sup>.

Preceding seismic events, the accumulation of stress in tectonic plates induces to generation of diverse anomalies in the designated earthquake preparation zone, represented as earthquake precursors<sup>[12]</sup>. Presently, one of the most efficacious precursors lies in anomalies relating to ionospheric parameters, exemplified by alterations in the vertical total electron content

(VTEC or TEC) in the ionosphere<sup>[13, 14]</sup>. This investigation has been predicated upon TEC anomalies utilization.

The nations Haiti, Dominican, and the Jamaica Republic are positioned across the Enriquillo–Plantain Garden Fault Zone (EPGFZ), which represents a significant left-lateral, strike-slip fault system delimiting the boundaries of the Caribbean and North American tectonic plates<sup>[15-17]</sup>. On January 12, 2010, Haiti experienced a major earthquake ( $M_L$  7.0), constituting the most significant occurrence in the southern region of Hispaniola since 1751<sup>[17, 18]</sup>, which also inflicted severe damage upon Port-au-Prince. This catastrophe led to the tragic loss of over 200,000 lives and resulted in an estimated 8 to 13 billion United States dollars in damages, equivalent to the entirety of the nation's gross domestic product, and approximately one-third of the overall population, has been affected by the earthquakes<sup>[19]</sup>. This study focuses on assessing the combined effects of seismic activity in conjunction with meteorological data from terrestrial sources<sup>[20]</sup>, as well as geomagnetic and solar activity such as the global geomagnetic activity ( $K_p$ -index), and the disturbance time storms ( $D_{st}$ ) parameters from the upper atmosphere side on the TEC variation<sup>[21-23]</sup>.

The appearance of the precursors studied varies from earthquake to earthquake depending on the time, location and magnitude of the earthquakes, so there is still a great need for more research in

\* Corresponding author

E-mail address: [marjan.ghafar@uoh.edu.iq](mailto:marjan.ghafar@uoh.edu.iq) (Instructor).

Peer-reviewed under the responsibility of the University of Garmian.

this area, especially for a major earthquake like the one in Haiti. This study will examine the vertical-TEC perturbations for several days leading up to and following the devastating earthquake in Haiti in the EPGFZ. The significance of this research lies in the statistical correlations established between the atmospheric parameters and TEC perturbations, the results of these studies are critical for validating the coupling models and could enhance essential insights into earthquake prediction within the EPGFZ and other seismologically active regions worldwide.

## 2. Data and Statistical Analysis

### 2.1 Study Area

The Caribbean region positioned within the southern expanse of the Middle American Ocean, constitutes an integral part of the Atlantic Ocean, geographically delimited by Central, North, and South America, as well as Haiti, and Jamaica<sup>[24]</sup>. The interior region of the Caribbean Plate demonstrates an east-northeastward movement at an angle of 70 degrees east of true north, with a velocity ranging between 18 to 20 mm per year relative to the North American Plate<sup>[25]</sup>. The oblique convergence of tectonic forces in the region is characterized by distinct components of proximal strike-slip and thrust movement. Specifically, the Enriquillo–Plantain Garden fault zone (EPGFZ) at a rate of  $7 \pm 2$  mm per year<sup>[26]</sup>.

The seismic event that occurred on January 12, 2010, registering a magnitude of  $M_L 7.0$ , stands as the most significant seismic occurrence in the southern sector of Hispaniola since the notable events transpired on September 15, 1751. The earthquake inflicted severe damage upon the city of Port-au-Prince metropolitan area, the capital city of Haiti. The study area for this research is the Enriquillo Plantain Garden Fault Zone (EPGFZ) as shown in Figure 1 (A, and B)<sup>[27, 28]</sup>.

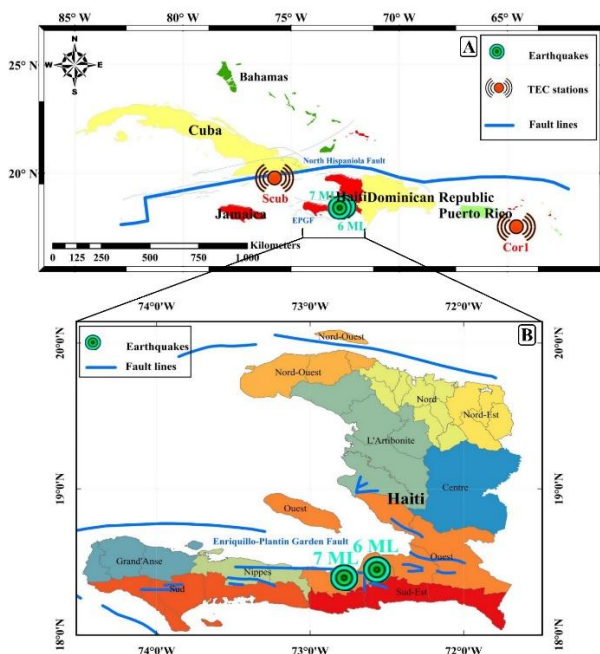


**Figure 1:** (A) Plate Boundaries and Faults in the Caribbean-North America Region: Including Surrounding Countries. (B) Surface trace, major active plate-boundary faults (blue lines), and seismicity in the Enriquillo-Plantain Garden Fault Zone (EPGFZ).

The details of the major earthquake were downloaded from the United States Geological Survey (USGS) through the website (<https://earthquake.usgs.gov/earthquakes/search/>). The seismic events that occurred inside the Earthquake Prediction Zone (EPZ) of the major earthquake are included in the acquiring data, Table 1 includes detailed information about earthquakes.

### 2.2 VTEC data

The vertical-TEC data was extracted from the Ionospheric Research Laboratory (IONOLAB) -Türkiye through (<http://www.ionolab.org/index.php?page=ionolabtec&language=en>). The IONOLAB employs the regularized estimation method to the Global Positioning System (GPS) measurements to obtain vertical-TEC (VTEC) values for mid-latitude stations at 2.5-minute intervals and publish them in TECU. One TECU quantifies about  $10^{16}$  electrons per square meter ( $m^2$ )<sup>[29]</sup>. The Dobrovolsky equation, expressed as preparation zone =  $(10^{0.43M_L})$ , was utilized to accurately estimate the EPZ radius of the major earthquake. This equation establishes a direct relationship between earthquake magnitude ( $M_L$ ) on the Richter scale and the corresponding preparation zone<sup>[30]</sup>. This study analyses the TEC for two stations namely, Santiago de Cuba in Cuba (Scub) located (latitude: 20.012, longitude: -75.762) inside the EPZ of the major earthquake, and Christiansted Virgin Islands in the U.S.A (Crol) (latitude: 17.757, longitude: -64.584) for the period of 28-12-2009 to 23-01-2010. In addition, VTEC can be influenced by the geomagnetic activities. To distinguish the seismicgenic with geomagnetic generated VTEC variations two more geomagnetic activities are considered: the global geomagnetic activity ( $K_p$ -index), and disturbance time storms ( $D_{st}$ ). these parameters' data were downloaded from the OMNI internet-based data repository, which is part of NASA's Explorer system project<sup>[31]</sup>. Access to essential information on geomagnetic activity and space weather is made simple by this database. With values ranging from 1 to 9, the  $K_p$ -index specifically acts as a measure of the solar wind-related disturbances in the Earth's magnetic field. In this study, a calm state is defined as one with a  $K_p$ -index value below 4<sup>[32]</sup>. The amount of geomagnetic activity over one hour is revealed by disturbance time storms ( $D_{st}$ ). It is considered a calm geomagnetic state if the  $D_{st}$  value is between -20 and 20 nT. These numbers serve as a benchmark for comparison for determining the magnitude of magnetic field disruption on Earth<sup>[33, 34]</sup>.

### 2.3 Statistical Analysis

Several methods have been used to detect anomalies in time series data like VTEC, for example, single parameter (univariate) forecasting models such as the ARIMA model<sup>[35,36]</sup>, multivariate models<sup>[37]</sup> and artificial intelligence<sup>[38, 39]</sup>. It seems that each of these models requires a lot of time and expertise to train and find the best model. That is why the method of mean and standard deviation was relied upon in this work. This method seems to be easier to use and more reliable, especially in this work where data ten days before and ten days after were used to determine the upper and lower limits for each single day using the following equations<sup>[20]</sup>.

$$\text{Upperlimit} = \mu(VTEC) + 2.\text{std}(VTEC)$$

$$\text{Lowerlimit} = \mu(VTEC) - 2.\text{std}(VTEC)$$

For each of these days, data from 10 days before and 10 days after were used to construct the upper and lower limits at that time for example, to build the upper limit for VTEC at 10 AM on 1-1-2010 the VTEC data at 10 AM from (December 22-31, 2009) and (January 2-12, 2010) were used<sup>[7, 40]</sup>. Whenever the daily VTEC falls above the upper bound, it is identified as a positive VTEC anomaly, while if it is less than the lower limit, it is identified as a negative VTEC anomaly. The following equations are used to determine the amount of anomalies.

$$Pos. dVTEC = VTEC(t) - (Upperbound - VTEC)$$

$$Neg. dVTEC = (Lowerbound - VTEC) - VTEC(t)$$

To eliminate the effect of the atmosphere on tech. The degree of proportionality between the tech and each of the atmospheric parameters was calculated as follows:

**Kendall's τ (tau) Formulation:**

Kendall's τ is a non-parametric test that measures the strength and direction of a monotonic relationship between two variables. It is calculated using the following formula:

$$\tau = \frac{\text{Number of concordant pairs} - \text{Number of discordant pairs}}{\text{Total number of pairs}}$$

**Spearman's ρ (rho) Formulation:**

Spearman's rank correlation coefficient is another non-parametric measure of the strength and direction of monotonic relationships. It is computed using the following formula:

$$\rho = 1 - \frac{6 \sum d_i^2}{n(n^2 - 1)}$$

Where:  $d_i$  represents the difference in ranks between corresponding pairs of observations, and  $n$  is the number of pairs of observations.

**Pearson Correlation Coefficient Formulation:**

The Pearson correlation coefficient is a parametric measure of the linear relationship between two variables. It is calculated using the following formula:

$$r = \frac{\sum (X_i - \bar{X})(Y_i - \bar{Y})}{\sqrt{(\sum (X_i - \bar{X})^2)(\sum (Y_i - \bar{Y})^2)}}$$

Where:  $X_i$  and  $Y_i$  are the individual observations in the datasets  $X$  and  $Y$ .  $\bar{X}$  and  $\bar{Y}$  are the means of the  $X$  and  $Y$  datasets, respectively. These formulations provide a quantitative measure of the relationships between variables based on different statistical approaches, allowing researchers to assess associations in their data.

**3. Results and Discussion**

In this study, the primary focus lies in the wide-ranging examination of the effects stemming from both seismic perturbations beneath the Earth's surface and geomagnetic activities in the upper atmosphere. Specifically, the aim is to discern potential correlations with variations in TEC in the ionosphere, a parameter of paramount importance in earthquake precursory research within the Enriquillo Plantain Garden Fault Zone. Notably, the TEC data was analyzed alongside records of geomagnetic and solar activities spanning from December 28, 2009, to January 23, 2010, before and after seismic activities.

To ensure a robust TEC data anomaly analysis, it thoroughly examined both upper and lower limits. Using a stringent calculation approach involving the mean and two standard deviations ( $\mu \pm 2\sigma$ ), for time spanning 26 days: 15 days before the seismic event and 10 days after. This method helps to indicate significant TEC variations. An evaluation of the literature, as represented in<sup>[7, 41]</sup>.

Intriguingly, a discernible alteration in TEC data occurred on January 13, 2010, preceding the seismic events registering (7.0  $M_L$  and 6.0  $M_L$ ) on the Richter scale as shown in Figure 2.

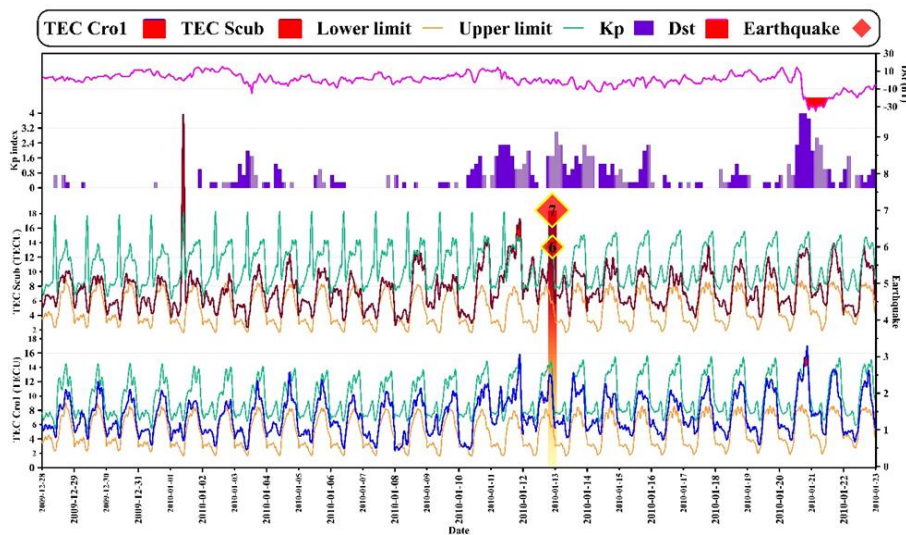


**Figure 2:** Exploring Fluctuations in Total Electron Content Leading Up to Macro-Earthquakes: Emphasizing Upper and Lower Confidence Intervals and the Influence of Solar and Geomagnetic Factors

Noteworthy increments were observed in the ionosphere, particularly within the 11 days' antecedent to the earthquakes by

13 TECU over the upper boundary. Additionally, a marginal elevation in TEC was noted a mere day prior to both seismic

occurrences more than (2 TECU), conspicuously evident at both TEC monitoring stations. Importantly, the surge surpassed the threshold set at  $(\mu \pm 2\sigma)$ , reaching an approximate value of 30 TECU at the Scub station. Because the  $K_p$  index and  $D_{st}$  parameters remain within the normal range, this anomalous surge is attributed to tectonic plate activity, wherein tectonic plate pressure culminates in the release of radon gas. The prevailing theory suggests that the emanation of radon (Rn) gas from epicentral regions plays a significant role in atmospheric ionization, as documented in the literature<sup>[42, 43]</sup>. This radioactive, colourless, and tasteless noble gas permeates seawater or soil<sup>[44]</sup>, eventually infiltrating the atmosphere, where it ionizes particles and augments atmospheric TEC content. This mechanism holds significant promise for pre-earthquake prognostication. This is attributed to radon's ability to prompt atmospheric ionization<sup>[45]</sup>. The presence of radon-generated ions in the air is believed to cause an upward movement of the upper ionosphere, where they migrate toward the lower ionosphere. Several satellite measurements have confirmed this phenomenon in the epicentral regions before seismic events. This suggests that TEC anomalies are valuable seismic precursors at specific locations<sup>[46]</sup>.

On December 31, 2009, the observed precipitation rate within 24 hours around Cor1 station resulted in the accumulation of surface

**Table 1:** Earthquake Data including Date, Magnitude, and Preparation Zone in the Study Area.

Date and Time	Lat	Long	Depth (km)	Mag	Preparation zone (km)	Distance from (Cro1) km	Distance from (Scub) km
12-01-2010 21:53	18.443	-72.571	13	7	1023.29	847.7	377.80
12-01-2010 22:00	18.387	-72.784	10	6	380.19	869.8	361.23

To extensively evaluate the intricate interplay between ionospheric variations and meteorological data from the same geographical locale both TEC stations (Scub, and Cor1) were accurately examined. These invaluable datasets were sourced from the reputable "POWER Data Access Viewer v2.0" and encompass a range of pivotal meteorological parameters, including precipitation levels, atmospheric temperature, surface air pressure, humidity levels, and wind speed. The meteorological data played a crucial role in understanding how atmospheric conditions affect the movement and release of radon gas from the Earth's surface into upper atmospheric layers leading to increased ionization rate. The meteorological parameters for the Crol (17.757, -64.584) station are shown in Figure 3.

The study observed stable conditions in key meteorological parameters such as specific humidity, atmospheric temperature, and surface pressure over the observation period. However, there was a notable increase in precipitation rate (approximately 0.8 mm/hour) recorded one day after a seismic event. The correlation between parameters is displayed in Table 2.

The meteorological parameters during the observation time for Scub station (20.012, -75.762) are shown in Figure 4.

At the Scub station, the majority of meteorological parameters exhibited a remarkable degree of stability. However, a slight deviation was observed in specific humidity, which reached its nadir 24 hours prior to the seismic event. Additionally, a marginal uptick in wind speed was noted over the same period. These

water, saturating soil pores, and blocking radon gas emanation. This phenomenon delays the release of radon gas into the atmosphere, subsequently impacting ionization rates and Total Electron Content (TEC) variations<sup>[7]</sup>. As a consequence, TEC values at the Cor1 station persist within the approximate normal range compared to the Scub station TEC anomaly. This discrepancy elucidates the TEC surge observed on January 20, 2010, one week after seismic activity at the Cor1 station. The surge, exceeding the upper-level threshold by 1.75 TECU, is ascribed to variances in the disturbance time storms ( $D_{st}$ ) parameter, plummeting to below -20 nT, constituting an anomalous reading. These fluctuations are posited to have exerted a discernible influence on TEC variations. The  $K_p$ - indicates a normal level during the observation period.

Another crucial factor considering the spatial separation between earthquake epicentres and TEC stations, a thorough assessment (Table 1) shows both events are roughly twice as far from Cor1 compared to Scub. Consequently, Cor1's readings seem normal. Also, Cor1 is outside the earthquake preparation zone based on the Dobrovolsky calculation, supporting the idea that the absence of TEC anomalies is likely due to these factors.

observations highlight the dynamic nature of atmospheric conditions preceding seismic events.

This study employed three correlation coefficient tests (Kendall's tau, Spearman's rho, and Pearson) to assess robustness, parameter intensity, direction, and effect sizes related to each other. This analytical framework enabled a comprehensive evaluation of all parameters.

Spearman's rho ( $\rho$ ) gauges the intensity and direction of a monotonic association between two variables<sup>[47]</sup>. Monotonicity entails a consistent ascending or descending pattern, not strictly linear. Like the Pearson correlation, it ranges from -1 to +1. Kendall's tau ( $\tau$ ) serves as another metric for evaluating the strength and direction of a monotonic correlation between two variables<sup>[48]</sup>. It bears resemblance to Spearman's rho and shares a -1 to +1 range, denoting perfect negative or positive monotonic relationships, with 0 indicating none. Kendall's tau, akin to Spearman's rho, does not presume linearity and applies to variables with non-normal distributions<sup>[49]</sup>. The parameters correlation coefficient is shown in the **Table 2**.

**Table 2.** displays correlation coefficients between TEC (Total Electron Content) and various meteorological variables (Temperature, Humidity, Precipitation, Surface Pressure, and Wind Speed) using three different correlation methods: Kendall's  $\tau$ , Spearman's  $\rho$ , and Pearson.

**Table 2:** Correlation Coefficients for Robustness, Intensity, and Direction of Parameters: Pearson, Spearman's ( $\rho$ ), and Kendall's ( $\tau$ ) Analysis.

Correlations							Descriptive Statistics			
Cro1 TEC station			Temperature	Humidity	Precipitation	Surface Pressure	Wind Speed		Mean	Std. Deviation
Kendall's ( $\tau$ )	TEC	Correlation Coefficient	-0.105	0.188	0.188	0.225	0.136	TEC (cor1)	7.34	0.81
		Sig. (2-tailed)	0.453	0.179	0.184	0.108	0.332	Temperature	26.54	0.42
Spearman's ( $\rho$ )	TEC	Correlation Coefficient	-0.185	0.248	0.244	0.361	0.177	Humidity	16.60	0.73
		Sig. (2-tailed)	0.365	0.222	0.229	0.070	0.387	Precipitation	0.04	0.06
Pearson	TEC	Correlation Coefficient	-0.147	0.291	0.241	0.314	0.032	Surface Pressure	101.60	0.13
		Sig. (2-tailed)	0.473	0.150	0.235	0.118	0.877	Wind Speed	5.04	1.84
Scub TEC station			Temperature	Humidity	Precipitation	Surface Pressure	Wind Speed		Mean	Std. Deviation
Kendall's ( $\tau$ )	TEC	Correlation Coefficient	0.046	0.132	-0.188	0.108	0.089	TEC (scub)	7.62	0.96
		Sig. (2-tailed)	0.741	0.343	0.233	0.440	0.523	Temperature	23.73	1.64
Spearman's ( $\rho$ )	TEC	Correlation Coefficient	0.099	0.158	-0.237	0.183	0.155	Humidity	13.49	1.61
		Sig. (2-tailed)	0.631	0.442	0.244	0.371	0.450	Precipitation	0.01	0.03
Pearson	TEC	Correlation Coefficient	-0.291	-0.187	-0.070	0.333	0.315	Surface Pressure	99.77	0.20
		Sig. (2-tailed)	0.150	0.359	0.733	0.097	0.117	Wind Speed	4.30	1.32
							*. Correlation is significant at the 0.05 level (2-tailed).      **. Correlation is significant at the 0.01 level (2-tailed).			

Kendall's ( $\tau$ ) Correlation: For TEC (Cro1) and Temperature, the correlation coefficient is (-0.105), which indicates a weak negative correlation. However, the p-value significant is 0.453, suggesting that this correlation is not statistically significant. For TEC (Cro1) and Humidity, the correlation coefficient is 0.188, indicating a weak positive correlation. Again, the p-value is 0.179, indicating a lack of statistical significance. Similarly, for Precipitation, Surface Pressure, and Wind Speed, the correlations are weak, and none of them are statistically significant.

The results from Spearman's correlation are similar to Kendall's  $\tau$ , with slightly different correlation coefficients and p-values. None of the correlations are statistically significant.

Pearson Correlation: For TEC (Cro1) and Temperature, the correlation coefficient is -0.147, indicating a weak negative correlation. The p-value is 0.473, indicating that this correlation is not statistically significant. For Precipitation, Humidity, Surface Pressure, and Wind Speed, the correlations are weak, and none of them are statistically significant.

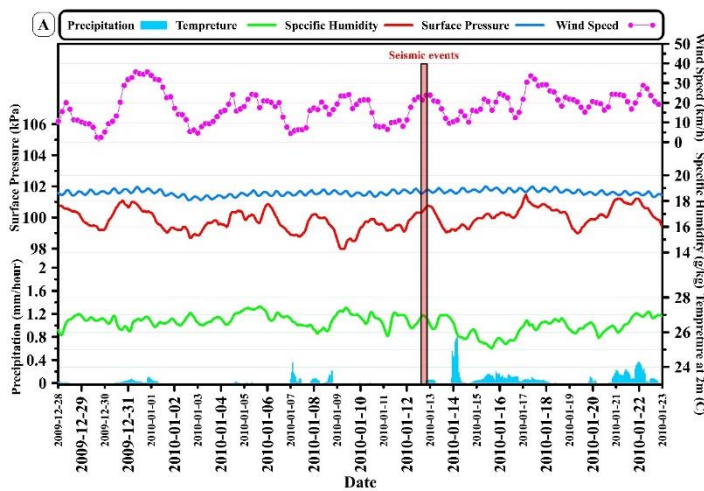


**Figure 3:** Meteorological Parameters Surrounding Cor1 TEC station.

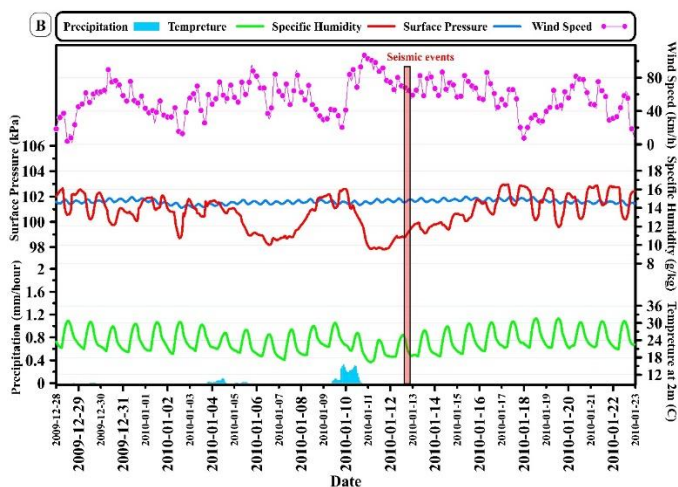


**Figure 4:** Meteorological Parameters Surrounding Scub TEC station.

## Conclusions

This research has systematically explored the complex interplay between subterranean seismic disturbances, geomagnetic phenomena in the upper atmosphere, and their consequential impacts on Total Electron Content (TEC) in the ionosphere. The comprehensive investigation entailed a detailed analysis of TEC data, augmented by assessments of geomagnetic, solar activities, and meteorological influences, during a pivotal timeframe encompassing two notable seismic episodes in the Enriquillo Plantain Garden Fault Zone.

A salient finding of this study was the marked modulation in TEC readings antecedent to these seismic occurrences, suggesting a plausible linkage. This prominent deviation in TEC values, particularly pronounced at the Scub station, was deduced to be the result of radon gas emissions ensuing from pre-seismic tectonic movements. The substantial spatial separation of the Cor1 station from the earthquake epicentres, in conjunction with its positioning beyond the demarcated earthquake preparatory zone, elucidated the non-observation of TEC anomalies there. Nonetheless, the correlation analyses unveiled a negligible and largely ineffective relationship between meteorological variables and TEC alterations at both monitoring sites.

Overall, the findings of this research underscore the significant role of ionospheric TEC variations as indicators for earthquake prediction. Furthermore, they underscore the imperative need for holistic and integrative approaches in the development of comprehensive earthquake prediction methodologies. These insights serve as a cornerstone for future endeavours in the realm of seismo-ionospheric research, potentially revolutionizing our approach to seismic hazard assessment and mitigation strategies.

## Author Contributions

**Marjan Mohammed Ghafar:** Conceptualization, methodology, formal analysis, and writing.

**Sarkhel Dleer:** Data collection, methodology, and writing.

**Sebar Mukhtar:** Data collection and methodology.

**Dawar Hama Khalid Mohammed:** Data analysis, creation of graphs, and methodology.

**Hemn Salh:** Review, supervision, and critical input.

## Funding

The authors received no financial support for the research, authorship, and publication of this article.

## Conflicts of Interest

None

## Acknowledgements

The Electrical and Electronics Engineering Department of Hacettepe University's IONOLAB (<http://www.ionolab.org/index.php?page=index&language=en>) appreciates our heartfelt thanks for providing us with the TEC data, which was essential in our research. We are also grateful to

the USGS Observatory for providing the seismic information (Earthquakes | U.S. Geological Survey (usgs.gov), which played a crucial role in our analysis. Additionally, we extend our appreciation to the OMNI internet-based data repository established by NASA OMNIWeb Data Explorer (nasa.gov), which provided us with access to valuable geomagnetic data, including the Kp index, Dst, and F10.7, and for POWER Data Access Viewer for providing meteorology data. (<https://power.larc.nasa.gov/data-access-viewer/>). We acknowledge the significant contribution of these organizations in enabling us to conduct our research. This research did not receive any specific grant from funding agencies in the public, commercial, or not-for-profit sectors.

## References

1. Y. Ogata, "Statistics of Earthquake Activity: Models and Methods for Earthquake Predictability Studies," *Annu Rev Earth Planet Sci*, vol. 45, no. 1, pp. 497–527, Aug. 2017, doi: 10.1146/annurev-earth-063016-015918.
2. J. B. Rundle, S. Stein, A. Donnellan, D. L. Turcotte, W. Klein, and C. Saylor, "The complex dynamics of earthquake fault systems: new approaches to forecasting and nowcasting of earthquakes," *Reports on Progress in Physics*, vol. 84, no. 7, p. 076801, Jul. 2021, doi: 10.1088/1361-6633/abf893.
3. R. J. Geller, D. D. Jackson, Y. Y. Kagan, and F. Mulargia, "Earthquakes cannot be predicted," *Science* (1979), vol. 275, no. 5306, p. 1616, 1997.
4. F. KÜLAHCI and Ş. ÇİÇEK, "Time-series analysis of water and soil radon anomalies to identify micro, macro earthquakes," *Arabian Journal of Geosciences*, vol. 8, no. 7, pp. 5239–5246, 2015.
5. A. Berhich, F.-Z. Belouadha, and M. I. Kabbaj, "A location-dependent earthquake prediction using recurrent neural network algorithms," *Soil Dynamics and Earthquake Engineering*, vol. 161, p. 107389, 2022.
6. M. Bhatia, T. A. Ahangar, and A. Manocha, "Artificial intelligence based real-time earthquake prediction," *Eng Appl Artif Intell*, vol. 120, p. 105856, 2023.
7. D. H. K. Mohammed, F. KÜLAHCI, and A. Muhammed, "Determination of possible responses of Radon-222, magnetic effects, and total electron content to earthquakes on the North Anatolian Fault Zone, Türkiye: an ARIMA and Monte Carlo Simulation," *Natural Hazards*, vol. 108, no. 3, pp. 2493–2512, 2021, doi: 10.1007/s11069-021-04785-8.
8. D. H. K. MOHAMMED, F. KÜLAHCI, and A. SAİT ALALI, "Evaluation of the Effects of Earthquakes on Radon and Total Electron Content Values and Meteorological Changes on the North Anatolian Fault Zone, Türkiye," *Turkish Journal of Science and Technology*, vol. 18, no. 1, Mar. 2023, doi: 10.55525/tjst.1184366.
9. S. Pulnests and K. Boyarchuk, *Ionospheric precursors of earthquakes*. Springer Science & Business Media, 2004.
10. W. Zhou, Y. Liang, X. Wang, Z. Ming, Z. Xiao, and X. Fan, "Introducing macrophages to artificial immune systems for earthquake prediction," *Appl Soft Comput*, vol. 122, p. 108822, 2022.
11. H. Le, L. Liu, J.-Y. Liu, B. Zhao, Y. Chen, and W. Wan, "The ionospheric anomalies prior to the M9.0 Tohoku-Oki earthquake," *J Asian Earth Sci*, vol. 62, pp. 476–484, 2013, doi: <https://doi.org/10.1016/j.jseae.2012.10.034>.
12. S. Pulnests and D. Ouzounov, *The Possibility of Earthquake Forecasting*. IOP Publishing, 2018.
13. D. Pundhir, B. Singh, and O. P. Singh, "Anomalous TEC variations associated with the strong Pakistan-Iran border region earthquake of 16 April 2013 at a low latitude station Agra, India," *Advances in Space Research*, vol. 53, no. 2, pp. 226–232, 2014.
14. M. R. Mansouri Daneshvar, M. Khosravi, and T. Tavousi, "Seismic triggering of atmospheric variables prior to the major earthquakes in the Middle East within a 12-year time-period of 2002–2013," *Natural hazards*, vol. 74, pp. 1539–1553, 2014.
15. B. Mercier de Lépinay et al., "The 2010 Haiti earthquake: A complex fault pattern constrained by seismologic and tectonic observations," *Geophys Res Lett*, vol. 38, no. 22, p. n/a-n/a, Nov. 2011, doi: 10.1029/2011GL049799.
16. C. M. McHugh et al., "Offshore sedimentary effects of the 12 January 2010 Haiti earthquake," *Geology*, vol. 39, no. 8, pp. 723–726, Aug. 2011, doi: 10.1130/G31815.1.
17. N. Saint Fleur, Y. Klinger, and N. Feuillet, "Detailed map, displacement, paleoseismology, and segmentation of the Enriquillo–Plantain Garden Fault in Haiti," *Tectonophysics*, vol. 778, p. 228368, Mar. 2020, doi: 10.1016/j.tecto.2020.228368.
18. C. S. Prentice et al., "Seismic hazard of the Enriquillo–Plantain Garden fault in Haiti inferred from palaeoseismology," *Nat Geosci*, vol. 3, no. 11, pp. 789–793, 2010.
19. E. Calais et al., "Transpressional rupture of an unmapped fault during the 2010 Haiti earthquake," *Nat Geosci*, vol. 3, no. 11, pp. 794–799, Nov. 2010, doi: 10.1038/ngeo992.
20. H. Salh, A. Muhammad, M. M. Ghafar, and F. KÜLAHCI, "Potential utilization of air temperature, total electron content, and air relative humidity as possible earthquake precursors: A case study of Mexico M7.4 earthquake," *J Atmos Sol Terr Phys*, vol. 237, p. 105927, Oct. 2022, doi: 10.1016/j.jastp.2022.105927.
21. M. Shah et al., "Total electron content anomalies associated with earthquakes occurred during 1998–2019," *Acta Astronaut*, vol. 175, pp. 268–276, 2020, doi: <https://doi.org/10.1016/j.actastro.2020.06.005>.
22. W. Fan, J. J. McGuire, C. D. de Groot-Hedlin, M. A. H. Hedlin, S. Coats, and J. W. Fiedler, "Stormquakes," *Geophys Res Lett*, vol. 46, no. 22, pp. 12909–12918, 2019.
23. F. T. Freund, M. R. Mansouri Daneshvar, and M. Ebrahimi, "Atmospheric Storm Anomalies Prior to Major Earthquakes in the Japan Region," *Sustainability*, vol. 14, no. 16, p. 10241, Aug. 2022, doi: 10.3390/su141610241.
24. S. Leroy, B. M. de Lépinay, A. Mauffret, and M. Pubellier, "Structural and tectonic evolution of the eastern Cayman Trough (Caribbean Sea) from seismic reflection data," *Am Assoc Pet Geol Bull*, vol. 80, no. 2, pp. 222–247, 1996.
25. P. Mann, E. Calais, J. Ruegg, C. DeMets, P. E. Jansma, and G. S. Mattioli, "Oblique collision in the northeastern Caribbean from GPS measurements and geological observations," *Tectonics*, vol. 21, no. 6, Dec. 2002, doi: 10.1029/2001TC001304.
26. D. M. Manaker et al., "Interseismic plate coupling and strain partitioning in the northeastern Caribbean," *Geophys J Int*, vol. 174, no. 3, pp. 889–903, 2008.
27. P. Mann, E. Calais, J. Ruegg, C. DeMets, P. E. Jansma, and G. S. Mattioli, "Oblique collision in the northeastern Caribbean from GPS measurements and geological observations," *Tectonics*, vol. 21, no. 6, pp. 1–7, 2002.
28. E. Calais and B. M. De Lépinay, "Semi-quantitative modeling of strain and kinematics along the Caribbean/North America strike-slip plate boundary zone," *J Geophys Res Solid Earth*, vol. 98, no. B5, pp. 8293–8308, 1993.
29. A. Muhammad, F. KÜLAHCI, and S. Birel, "Investigating radon and TEC anomalies relative to earthquakes via AI models," *J Atmos Sol Terr Phys*, vol. 245, p. 106037, Apr. 2023, doi: 10.1016/j.jastp.2023.106037.
30. I. P. Dobrovolsky, S. I. Zubkov, and V. I. Miachkin, "Estimation of the size of earthquake preparation zones," *Pure Appl Geophys*, vol. 117, no. 5, pp. 1025–1044, 1979.
31. P. Tucio, E. Macalalad, R. M. Guido, J. Kalaw, and P. P. Divinagracia, "Ionospheric Precursor Associated to the 2012 Sumatra Earthquake Observed over the Taiwan-Philippines Region using GNSS-TEC," in *2021 7th International Conference on Space Science and Communication (IconSpace)*, IEEE, Nov. 2021, pp. 202–206. doi: 10.1109/IconSpace53224.2021.9768729.
32. M. Menvielle and A. Berthelier, "The K-derived planetary indices: Description and availability," *Reviews of Geophysics*, vol. 29, no. 3, pp. 415–432, 1991.
33. L. R. Cander and S. J. Mihajlovic, "Forecasting ionospheric structure during the great geomagnetic storms," *J Geophys Res Space Phys*, vol. 103, no. A1, pp. 391–398, 1998.
34. J. H. King and N. E. Papitashvili, "Solar wind spatial scales in and comparisons of hourly Wind and ACE plasma and magnetic field data," *J Geophys Res Space Phys*, vol. 110, no. A2, 2005.
35. Y. Kong, H. Chai, J. Li, Z. Pan, and Y. Chong, "A modified forecast method of ionosphere VTEC series based on ARMA model," in *2017 Forum on Cooperative Positioning and Service (CPGPS)*, IEEE, 2017, pp. 90–95.
36. F. Ahmed and monem mohammed, "A Forecasting Time Series model Based on Entropy and Fuzzy logic," *Passer Journal of Basic and Applied Sciences*, vol. 5, no. 2, pp. 304–310, Jul. 2023, doi: 10.24271/psr.2023.381058.1230.
37. D. V. Ratnam, Y. Otsuka, G. Sivavaraprasad, and J. R. K. K. Dabbakuti, "Development of multivariate ionospheric TEC forecasting algorithm using linear time series model and ARMA over low-latitude GNSS station," *Advances in Space Research*, vol. 63, no. 9, pp. 2848–2856, 2019.
38. A. Muhammad, F. KÜLAHCI, and S. Birel, "Investigating radon and TEC anomalies relative to earthquakes via AI models," *J Atmos Sol Terr Phys*, vol. 245, p. 106037, Apr. 2023, doi: 10.1016/j.jastp.2023.106037.
39. A. Guron, M. Anwer, S. Sulaiman, and S. AbdulSamad, "Classification of the cause of eye impairment using different kinds of machine learning

- algorithms,” *Passer Journal of Basic and Applied Sciences*, vol. 5, no. 2, pp. 410–416, Nov. 2023, doi: 10.24271/psr.2023.397078.1328.
40. M. Shah, M. A. Tariq, J. Ahmad, N. A. Naqvi, and S. Jin, “Seismo ionospheric anomalies before the 2007 M7.7 Chile earthquake from GPS TEC and DEMETER,” *J Journal of Geodynamics*, vol. 127, pp. 42–51, 2019.
  41. M. Shah, M. A. Tariq, J. Ahmad, N. A. Naqvi, and S. Jin, “Seismo ionospheric anomalies before the 2007 M7.7 Chile earthquake from GPS TEC and DEMETER,” *J Geodyn*, vol. 127, pp. 42–51, 2019, doi: 10.1016/j.jog.2019.05.004.
  42. J. R. Holliday, K. Z. Nanjo, K. F. Tiampo, J. B. Rundle, and D. L. Turcotte, “Earthquake forecasting and its verification,” *Nonlinear Process Geophys*, vol. 12, no. 6, pp. 965–977, 2005.
  43. M. Hayakawa, A. Schekotov, J. Izutsu, S.-S. Yang, M. Solovieva, and Y. Hobara, “Multi-parameter observations of seismogenic phenomena related to the Tokyo earthquake (M= 5.9) on 7 October 2021,” *Geosciences (Basel)*, vol. 12, no. 7, p. 265, 2022.
  44. O. Baykara, M. Inceöz, F. Külahcı, M. Doğru, and E. Aksoy, “Assessment of <sup>222</sup>Rn concentration and terrestrial gamma-radiation dose rates in the seismically active area,” *J Radioanal Nucl Chem*, vol. 278, no. 1, pp. 59–63, Oct. 2008, doi: 10.1007/s10967-007-7237-5.
  45. G. Zhou, X. Bao, S. Ye, H. Wang, and H. Yan, “Selection of optimal building facade texture images from UAV-based multiple oblique image flows,” *IEEE Transactions on Geoscience and Remote Sensing*, vol. 59, no. 2, pp. 1534–1552, 2020.
  46. A. A. Namgaladze, M. V. Klimenko, V. V. Klimenko, and I. E. Zakharenkova, “Physical mechanism and mathematical modeling of earthquake ionospheric precursors registered in total electron content,” *Geomagnetism and Aeronomy*, vol. 49, pp. 252–262, 2009.
  47. C. Idosa and K. Shogile, “Effects of solar flares on ionospheric TEC over Iceland before and during the geomagnetic storm of 8 September 2017,” *Phys Plasmas*, vol. 29, no. 9, Sep. 2022, doi: 10.1063/5.0098971.
  48. A. Shekhovtsov, “How strongly do rank similarity coefficients differ used in decision making problems?,” *Procedia Comput Sci*, vol. 192, pp. 4570–4577, 2021.
  49. M. C. Bağdatlı and Y. Ballı, “The analysis of soil temperatures in different depths using spearman’s rho and mann-kendall correlation tests: the case study of Nigde center in Turkey,” 2020.